water

MDPI

Article

Age and Growth of *Hedinichthys yarkandensis* (Day, 1877) in the Hotan River

Xin-Yue Wang [1,2], Sheng-Ao Chen [1,2,*], Yong Song [1,2], Cheng-Xin Wang [1,2] and Fei Liu [1,2]

[1] College of Life Sciences and Technology, Tarim University, Alar 843300, China; 120050007@taru.edu.cn (X.-Y.W.)
[2] Tarim Research Center of Rare Fishes, Alar 843300, China
* Correspondence: shengao@taru.edu.cn; Tel.: +86-135-6767-6029

Abstract: *Hedinichthys yarkandensis* (Day, 1877) has been highlighted in research and evaluated as a class II key protected aquatic wildlife in Xinjiang Uygur Autonomous Region. To enhance the study of fish resources in the Hotan River, further germplasm conservation of fishery resources specific to the Tarim River Basin should be carried out, and the development of the aquatic seed industry should be promoted. A total of 1275 *H. yarkandensis* individuals were collected from 2020–2021. Fish ecological methods were used to explore the population ecological characteristics and ecological habits of *H. yarkandensis*. We found that the age of *H. yarkandensis* ranged from one to seven based on lapillus otoliths, and two-plus individuals accounted for more. The age structure composition reveals stable genetic performance and good population fecundity. The fitting correlations of standard length and body weight reveal that *H. yarkandensis* in the Hotan River is a uniformly growing fish. The ratio of females to males is 0.87:1. The Fulton condition index of males was slightly higher than that of females due to individual miniaturization. The comparative study found that the growth parameters of the Hotan River population (L_∞ = 302.772, W_∞ = 310.8450, t_0 = −0.4608) were higher than those of the other groups. The feeding demand of *H. yarkandensis* in the Hotan River was guaranteed because the effect of human activities was small in the watershed area and the watershed ecosystem was more stable, which resulted in stable germplasm resources in the Hotan River population.

Keywords: Hotan River; *H. yarkandensis*; age structure; growth characteristics

Citation: Wang, X.-Y.; Chen, S.-A.; Song, Y.; Wang, C.-X.; Liu, F. Age and Growth of *Hedinichthys yarkandensis* (Day, 1877) in the Hotan River. *Water* **2023**, *15*, 2948. https://doi.org/10.3390/w15162948

Academic Editor: Heiko L. Schoenfuss

Received: 24 June 2023
Revised: 5 August 2023
Accepted: 12 August 2023
Published: 16 August 2023

1. Introduction

The Hotan River is one of the three major sources of the Tarim River in China. It is formed by the convergence of the Yulong Kashi River, which originates from the northern slope of the Kunlun Mountains, and the Kara Kash, which originates from the northern slope of the Karakoram Mountains. As the largest river on the northern slope of the Kunlun Mountains, the Hotan River is recharged by alpine snow and ice melt and precipitation [1]. Most studies on the Hotan River have focused on soil and water resources and the ecological environment, including desertification on the southern edge of the Tarim Basin and climate change in southern Xinjiang [2–4]. Studies on the proliferation and conservation of endemic fishes of the Hotan River have not been reported, and fishery information is scarce.

Key wildlife conservation measures are put in place by the state. The protection level of wildlife is divided into national key protection, provincial key protection wildlife, and provincial general protection wildlife. *Triplophysa* (*Hedinichthys*) *yarkandensis* (Day, 1877), an endemic fish of the Tarim River system, is a class II key protected aquatic wildlife in Xinjiang Uygur Autonomous Region [5–7]. With the promotion of artificial propagation and conservation, the germplasm resources of *H. yarkandensis* have effectively recovered in recent years. The systematic study of basic biology benefits the development of conservation measures and has been coupled with the broad prospect of its increasing economic value. Hence, it is necessary to carry out multifaceted and wide-ranging studies on *H. yarkandensis*.

Research has focused on growth, reproduction, culture, toxicity testing, genetic diversity, and interspecific variation [8–11].

This study explored the age structure and growth characteristics of *H. yarkandensis* in the Hotan River based on fish ecology using continuous periodic sampling. The purpose was to analyze and evaluate the trend of fish population changes and to provide theoretical support for subsequent proliferation and conservation work.

2. Materials and Methods

2.1. Sample Collection

In total, 1275 *H. yarkandensis* individuals were collected (Table 1) using ground cages (mesh 2a = 2.00 cm) in four seasons from 2020 to 2021 in the Hotan River (Figure 1). The selected site is near the Red and White Mountains on the west bank of the lower Hotan River, which has a typical desert climate. It was determined that the gender ratio of the sample was 0.87:1. Biological determination was conducted on-site to the nearest 0.01 mm and 0.01 g [12]. Traditional morphological data included body depth (*BD*), body width (*BW*), head length (*HL*), snout length (*SL*), eye diameter (*ED*), eye interval (*EI*), length of caudal peduncle (*LCP*), and depth of the caudal peduncle (*DCP*) (Figure 2). The otoliths were removed by dissection and stored in PCR tubes containing 95% ethanol. The other tissues were fixed in a 10% formaldehyde solution and brought back to the laboratory for subsequent processing.

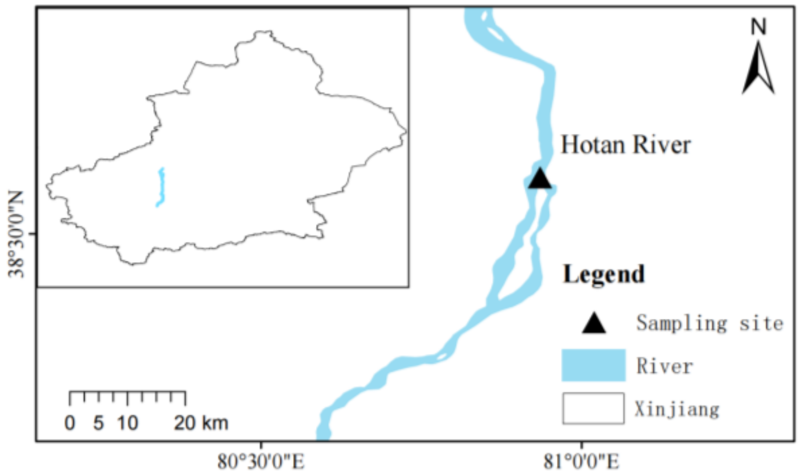

Figure 1. Sampling location of *H. yarkandensis*.

Figure 2. Morphological measurements of *H. yarkandensis*. 1. Total length; 2. Standard length; 3. Body depth; 4. Head length; 5. Snout length; 6. Eye diameter; 7. Length of caudal peduncle; 8. Depth of caudal peduncle.

Table 1. Sample information of *H. yarkandensis*.

Sampling Time	Sampling Site	Number	Standard Length/mm		Body Weight/g	
			Range	Mean ± S.D.	Range	Mean ± S.D.
2020.04 (spring)	E 80°80′ N 38°32′	326	67.72~177.24	104.60 ± 17.52	4.62~72.44	17.82 ± 10.26
2021.08 (summer)		311	51.82~131.42	70.68 ± 12.95	2.09~30.58	5.43 ± 3.68
2020.10 (autumn)		321	43.34~137.34	90.41 ± 13.49	1.09~35.11	11.06 ± 4.84
2021.01 (winter)		317	47.46~119.93	73.14 ± 12.51	0.91~22.95	5.79 ± 2.95

2.2. Otolith Characteristics

Otolith perimeter (*OP*), otolith area (*OA*), otolith length (*OL*), otolith width (*OW*), maximum radius of otolith (R_{max}), and minimum radius of otolith (R_{min}) were obtained by photographing and measuring with a body microscope (SMZ1270i) and NIS Element Viewer 4.2.0 software.

2.3. Age Identification

The lapillus otoliths of *H. yarkandensis* are relatively large and easily accessible. A subset of the sample (n = 100) of left and right lapillus otoliths was chosen at random for comparison. There was no significant difference between the left and right otoliths ($p > 0.05$); thus, the left lapillus otoliths were uniformly used for the analysis. The otoliths were fixed on slides with transparent nail polish and polished with sandpaper (600#~2000#) in a circular motion until clear whorls appeared. It was dissolved using acetone and then turned over after unilateral treatment. The above steps were repeated until the central nucleus of the otolith was clear [13].

The age was determined based on the number of annual whorls on the identification material. The first whorl served as the date of age progression. Each sample was independently identified by two or more observers using a light microscope. Readings were accepted only if the results of both observers were in agreement, and they were reidentified by a third person if they differed. If none of the results were consistent, the sample was discarded.

2.4. First-Round Confirmation and Annual Cycle of Formation

1. Otolith First-Round Confirmation

In this study, otolith microstructure analysis was carried out using the daily wheel counting method. The fish breeding season and the number of daily wheels of otoliths were used as the basis. The radius of otoliths of the recent *H. yarkandensis* juvenile samples and the hypothetical first wheel diameter of other fish older than 1 year were measured. The first wheel position was confirmed by comparing the above measurements [14,15].

2. Annual whorl formation cycle

In this study, marginal increment ratio (*MIR*) analysis was used to study the annual cycle formation of otoliths, which was calculated as follows [16]:

$$MIR = R - R_{\mathrm{n}}/R_{\mathrm{n}} - R_{\mathrm{n}-1}$$

where R: otolith radius; R_{n}: penultimate first whorl diameter; and $R_{\mathrm{n}-1}$: penultimate whorl diameter.

The otoliths were photographed under a body microscope (SMZ1270i) through an image acquisition system connected to a computer. Then, the otolith whorl diameter and counting day whorl were measured separately along the same direction of the caudal axis of the otoliths using NIS Element Viewer 4.2.0 software.

2.5. Growth Pattern

The power exponential relationship equation $W = aL^b$ was used to fit the relationship between standard length and body weight. a and b are the anisotropic growth parameters.

This method can be used to analyze fish growth characteristics. Testing the correlation difference between the b value and 3 by Pauly's t-test determined whether the fish had uniform growth or anisotropic growth [12,17].

Analysis of covariance (ANCOVA) was used for significance analysis [12]. The formula $K = W/L^3 \times 100{,}000$ was used to calculate the Fulton condition index. Fish abundance, nutritional status, growth traits, and environmental conditions were measured [18–20].

The standard length and body weight data were logarithmized and analyzed by analysis of covariance (ANCOVA) with $\ln W$ as a covariate to test whether there was a significant difference in the length-weight relationship between the sexes and to compare whether there was a significant difference in the anisotropic growth indexes b and 3 (the value of b in the isotropic state of growth) by using the Pauly-t test. The formula for the Pauly t-test was:

$$t = \frac{L_{\mathrm{SD}}}{W_{\mathrm{SD}}} \times \frac{|b-3|}{\sqrt{1-R^2}} \times \sqrt{n-2}$$

where L_{SD} is the standard deviation of the logarithmic value of body length; W_{SD} is the body standard deviation of the logarithmic value of weight; R^2 is the correlation coefficient; n is the number of samples.

2.6. Growth Equations, Growth Rate, and Growth Acceleration Equations

The growth equations for standard length and body weight were fitted using the von Bertalanffy approach to describe the age and growth characteristics [12,20]:

$$L_t = L_\infty(1 - \mathrm{e}^{-k(t-t_0)})$$

$$W_t = W_\infty\,(1 - \mathrm{e}^{-k\,(t-t_0)})$$

where L_t is the standard length of individual fish at age t; W_t is the body weight of individual fish at age t; L_∞ is the asymptotic standard length; W_∞ is the asymptotic body weight; t_0 is the age at which standard length and body weight are equal to zero in the theoretical state; and k is the average curvature of the growth curve.

To further predict the growth trend, first-order derivatives and second-order derivatives of the growth equations were calculated to obtain growth rates and growth accelerations [12,20]:

$$\mathrm{d}l/\mathrm{d}t = L_\infty k\mathrm{e}^{-k\,(t-t_0)}$$

$$\mathrm{d}W/\mathrm{d}t = bW_\infty k\mathrm{e}^{-k\,(t-t_0)}\,[1 - \mathrm{e}^{-k\,(t-t_0)}]^{b-1}$$

$$\mathrm{d}^2l/\mathrm{d}t^2 = -L_\infty k^2\mathrm{e}^{-k(t-t_0)}$$

$$\mathrm{d}^2W/\mathrm{d}t^2 = bW_\infty k^2\mathrm{e}^{-k\,(t-t_0)}\,[1 - \mathrm{e}^{-k\,(t-t_0)}]^{b-2}\,[b\,\mathrm{e}^{-k\,(t-t_0)} - 1]$$

where $\mathrm{d}l/\mathrm{d}t$ is the standard length growth rate; $\mathrm{d}W/\mathrm{d}t$ is the body weight growth rate; $\mathrm{d}^2l/\mathrm{d}t^2$ is the standard length growth acceleration; and $\mathrm{d}^2W/\mathrm{d}t^2$ is the body weight growth acceleration.

2.7. Relationship between Otolith Morphology and Standard Length and Body Mass

Linear, logarithmic, power, and exponential models were used to fit the relationship between the main morphological indicators of otoliths and the standard length and body mass of *H. yarkandensis*. The most appropriate model was chosen based on the Akaike information criterion (AIC) and was calculated as follows.

$$\mathrm{AIC} = n \times \ln(\mathrm{RSS}/n) + 2k$$

where k is the number of parameter constants in the equation; n is the number of samples; and RSS is the sum of squared residuals.

Software such as NIS Element Viewer 4.2.0, SPSS 18.0, and ORIGIN 9.0 were used to process the data.

3. Results

3.1. Otolith Morphology

The lapillus otolith of *H. yarkandensis* is tiny, roughly oval, that is, thick in the middle and gradually becoming thinner toward the edge, with a definite protrusion in the middle of the outer side. The intermajor groove is not visible, the basal lobe is well developed, the otolith abdominal edge is smooth and shallowly curved, and the otolith dorsum has a wave-like protrusion. The otolith length is much greater than the otolith breadth.

The left otolith was consistently employed in this investigation because the paired sample *t*-test revealed no significant difference between the morphology of the left and right lapillus otoliths of *H. yarkandensis* ($p > 0.05$).

The otolith area was 0.87 ± 0.18 mm^2, in the range of 0.39 to 1.54 mm^2; the otolith minimum radius was 0.86 ± 0.09 mm, in the range of 0.62 to 1.19 mm; the otolith maximum radius was 1.33 ± 0.15 mm, in the range of 0.85 to 1.75 mm; the otolith circumference was 3.58 ± 0.41 mm, in the range of 2.36 to 4.84 mm; the otolith length was 1.34 ± 0.20 mm, in the range of 0.86 to 2.66 mm; and the otolith width was 0.89 ± 0.13 mm, in the range of 0.62 to 1.83 mm.

3.2. Age Structure

In total, age identification was completed for 1245 of the 1275 samples (Table 2, Figure 3). The age group of the Hotan River population was 1~7 years old, and the dominant age was 2 years old.

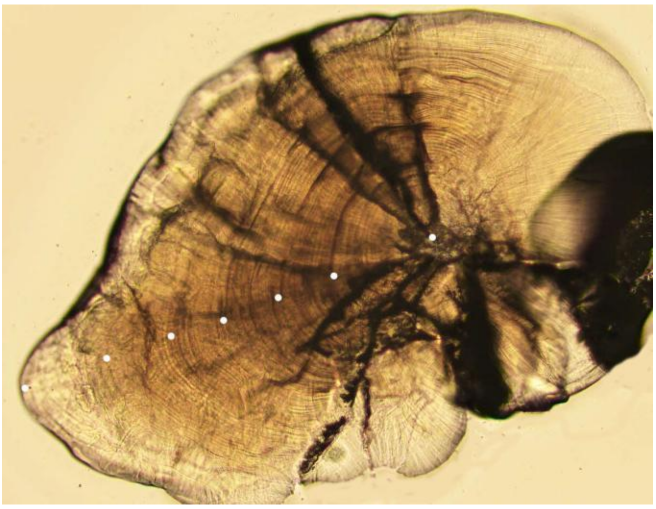

Figure 3. Annuli characteristics of lapillus otolith from *H. yarkandensis*.

Table 2. Age composition and structure of *H. yarkandensis*.

Age	*n*	Weight (g)		Length (mm)	
		Mean ± S.D.	Range	Mean ± S.D.	Range
1	236	2.98 ± 0.76	1.09–4.90	57.64 ± 4.21	43.34–63.49
2	627	5.94 ± 1.85	2.68–12.23	73.91 ± 7.29	63.51–90.21
3	291	14.58 ± 3.10	7.34–26.17	100.00 ± 5.80	90.24–111.26
4	76	25.92 ± 5.98	14.53–41.78	122.05 ± 8.61	111.33–141.70
5	13	52.09 ± 3.62	43.64–57.32	159.08 ± 6.05	148.61–170.51
6	1	71.73		171.21	
7	1	72.44		177.24	

3.3. First-Round Confirmation and Annual Round Formation Cycle

1. Otolith first-round confirmation

The otolith of *H. yarkandensis* consists of alternating bright and dark bands, and the distance of the daily whorl gradually narrows from the central nucleus to the edge. Nearly 1 year-old juveniles were selected, and their daily whorls were observed to be 52~176 (112.65 ± 15.74). The radius of the otoliths of these juveniles was 541.29 ± 90.72 µm. The mean whorl diameter of the hypothetical first whorl of samples above 1 year old was 561.92 ± 93.15 µm. This result confirms that the hypothetical first whorl of *H. yarkandensis* is accurate.

2. Annual whorl formation cycle

Figure 4 shows that the marginal growth rate of otoliths (*MIR*) had only one obvious peak from August to September and then decreased to the lowest point in October. This result indicated that the annual whorl formation cycle of otoliths was one year, and it formed from October through April.

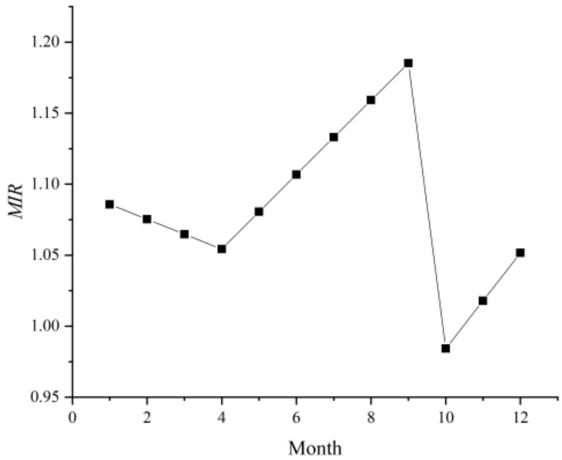

Figure 4. Monthly variation in the marginal growth rate of otoliths (*MIR*) in *H. yarkandensis*.

3.4. Distribution of Standard Length and Weight

Figure 5 shows that the standard length of the total population of *H. yarkandensis* in the Hotan River ranged from 43.34 to 177.24 mm and had a mean value of 80.65 ± 20.86 mm. The standard length of the male population ranged from 47.46 to 172.21 mm and had a mean value of 79.60 ± 20.83 mm. The standard length of the female population ranged from 43.34 to 177.24 mm and had a mean value of 81.82 ± 20.83 mm. The difference between male and female standard length was not significant ($p > 0.05$).

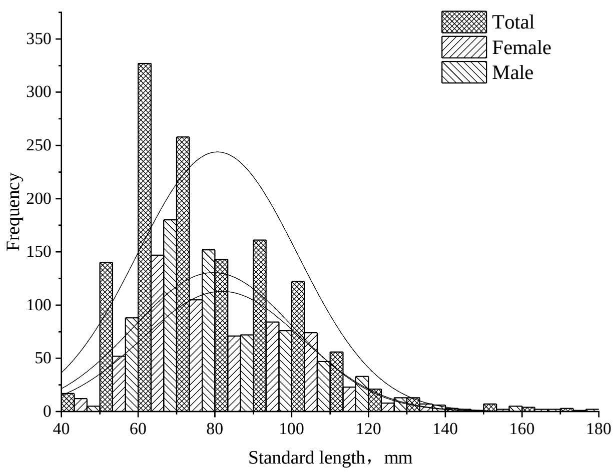

Figure 5. Standard length distribution of *H. yarkandensis* in the Hotan River.

Figure 6 shows that the body weight of the total population ranged from 1.09 g to 72.44 g, with a mean value of 9.12 ± 8.23 g. The body weight of the male population ranged from 1.25 g to 71.73 g, with a mean value of 8.92 ± 8.43 g. The body weight of the female population ranged from 1.09 g to 72.44 g, with a mean value of 9.34 ± 7.99 g. The difference between male and female body weight was not significant ($p > 0.05$).

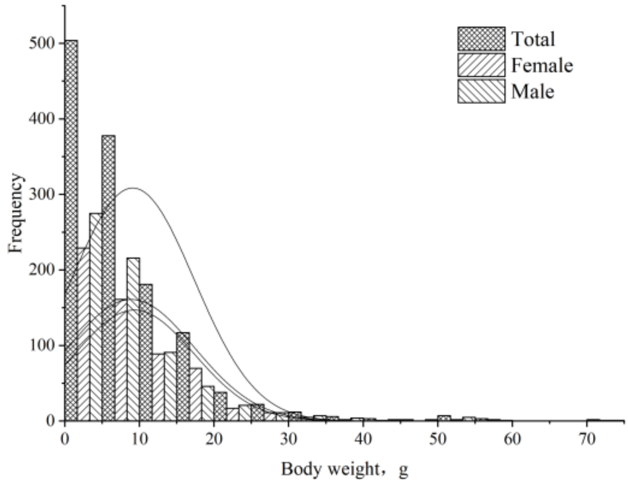

Figure 6. The body weight distribution of *H. yarkandensis* in the Hotan River.

3.5. Correlation Analysis of Standard Length and Body Weight

The correlation between standard length and body weight was fitted to the total population and the male and female populations of *H. yarkandensis* in the Hotan River by means of a power function relationship (Figure 7):

$$W_{\text{total}} = 2 \times 10^{-5} L^{2.8985}\ (R^2 = 0.9673, n = 1275)$$

$$W_{\text{male}} = 2 \times 10^{-5} L^{2.8768}\ (R^2 = 0.9668, n = 682)$$

$$W_{\text{female}} = 2 \times 10^{-5} L^{2.9283}\ (R^2 = 0.9683, n = 590)$$

The b values were significantly different from 3 ($t = 6.776$, $p < 0.05$). It should have indicated that it was an allometry growth fish. However, b values were between 2.5 and 4. Typically this means that *H. yarkandensis* was judged to be a uniformly growing fish.

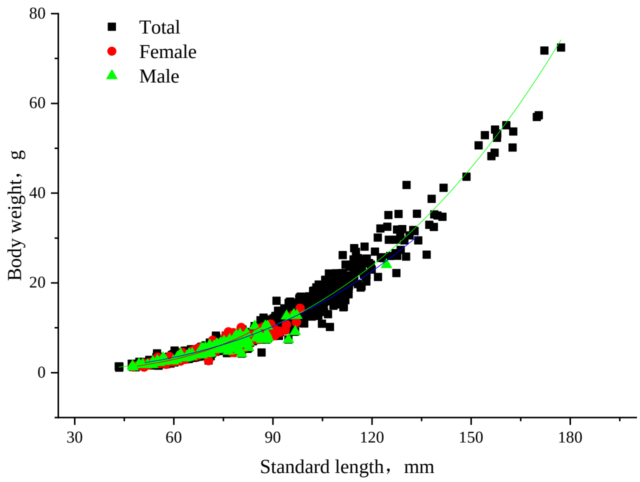

Figure 7. Length-weight relationship of *H. yarkandensis* in the Hotan River.

3.6. Fulton Condition Index

Figure 8 shows that the index of the *H. yarkandensis* population in the Hotan River was significantly higher in October. There was no significant difference between the male and female populations in the month group ($p > 0.05$). The mean Fulton condition index of males and females was 1.4654 and 1.4416, respectively. The total number of male fish was higher than that of female fish.

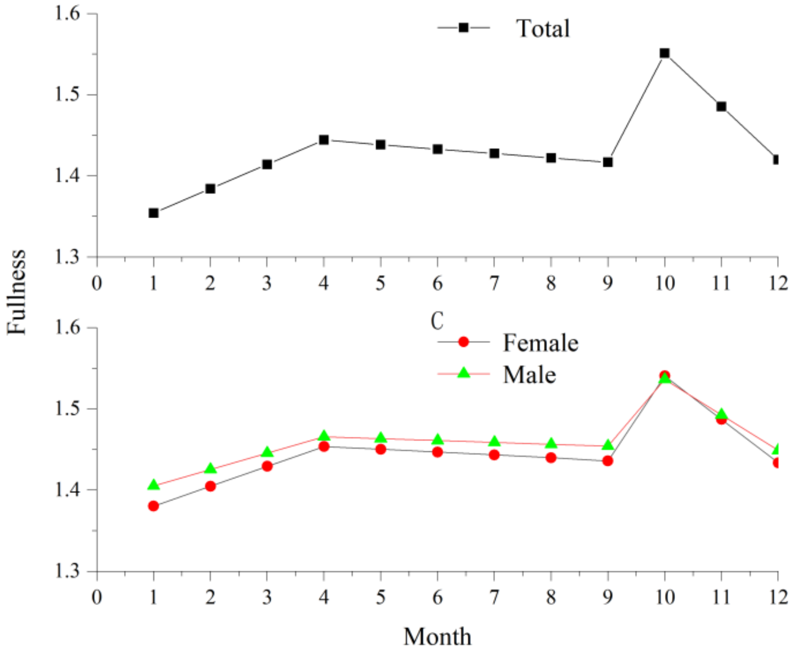

Figure 8. Variation in the Fulton condition index of *H. yarkandensis* in the Hotan River in different months.

3.7. Growth Equations, Growth Rate, and Growth Acceleration Equations

The growth equations, growth rate equations, and growth acceleration equations for the standard length and weight of different populations of *H. yarkandensis* were fitted as follows.

The total population of the Hotan River (Figure 9): L_∞ = 302.772, W_∞ = 310.8450, t_0 = −0.4608, and the inflection point age t_i was 9.0710 years.

$$L_t = 302.7720\,(1 - e^{-0.1117(t+0.4608)}),\ W_t = 310.8450\,(1 - e^{-0.1117(t+0.4608)})^{2.8985};$$

$$dL/dt = 33.8196\, e^{-0.1117(t+0.4608)},$$
$$dW/dt = 100.6399\, e^{-0.1117(t+0.4608)}\,(1 - e^{-0.1117(t+0.4608)})^{1.8985};$$

$$dL^2/dt^2 = -3.7777\, e^{-0.1117(t+0.4608)},$$
$$dW^2/dt^2 = 11.2415\, e^{-0.1117(t+0.4608)}\,(1 - e^{-0.1117(t+0.4608)})^{0.8985}\,(2.8985 \times e^{-0.1117(t+0.4608)} - 1).$$

The male population of the Hotan River was as follows (Figure 10): L_t = 301.5522 $(1 - e^{-0.1124(t+0.0098)})$, $W_t = 271.4314\,(1 - e^{-0.1124(t+0.0098)})^{2.8768}$, $dL/dt = 33.8945\, e^{-0.1124(t+0.0098)}$, $dW/dt = 87.7680\, e^{-0.1124(t+0.0098)}\,(1 - e^{-0.1124(t+0.0098)})^{1.8768}$, $dL^2/dt^2 = -3.8097\, e^{-0.1124(t+0.0098)}$, $dW^2/dt^2 = 9.8651\, e^{-0.1124(t+0.0098)}\,(1 - e^{-0.1124(t+0.0098)})^{0.8768}\,(2.8768 \times e^{-0.1124(t+0.0098)} - 1)$. The t_i was 9.3913 years.

The female population of the Hotan River was as follows (Figure 11): L_t = 306.5251 $(1 - e^{-0.1094(t+0.4958)})$, $W_t = 382.0749\,(1 - e^{-0.1094(t+0.4958)})^{2.9283}$, $dL/dt = 33.5338\, e^{-0.1094(t+0.4958)}$, $dW/dt = 122.4000\, e^{-0.1094(t+0.4958)}\,(1 - e^{-0.1094(t+0.4958)})^{1.9283}$, $dL^2/dt^2 = -3.6686\, e^{-0.1094(t+0.4958)}$, $dW^2/dt^2 = 13.3056\, e^{-0.1094(t+0.4958)}\,(1 - e^{-0.1094(t+0.4958)})^{0.9283}\,(2.9283 \times e^{-0.1094(t+0.4958)} - 1)$. The t_i was 9.3252 years.

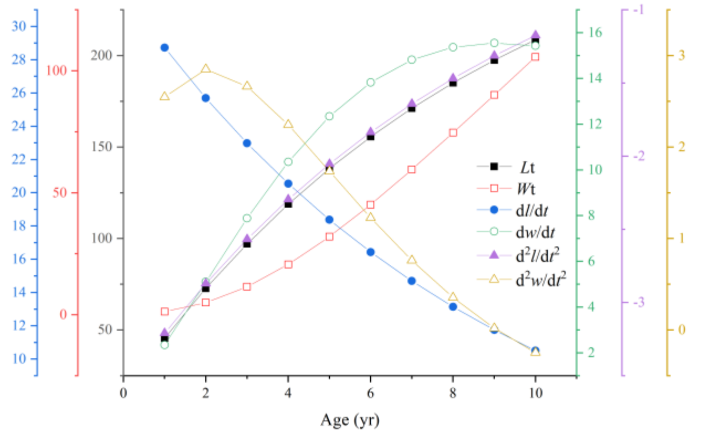

Figure 9. Von Bertalanffy growth/growth rate/growth acceleration of the standard length and weight of the total population in the Hotan River.

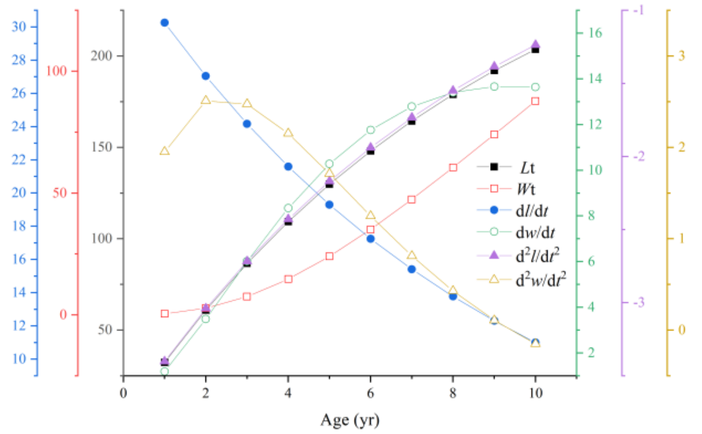

Figure 10. Von Bertalanffy growth/growth rate/growth acceleration of the standard length and weight of the male population in the Hotan River.

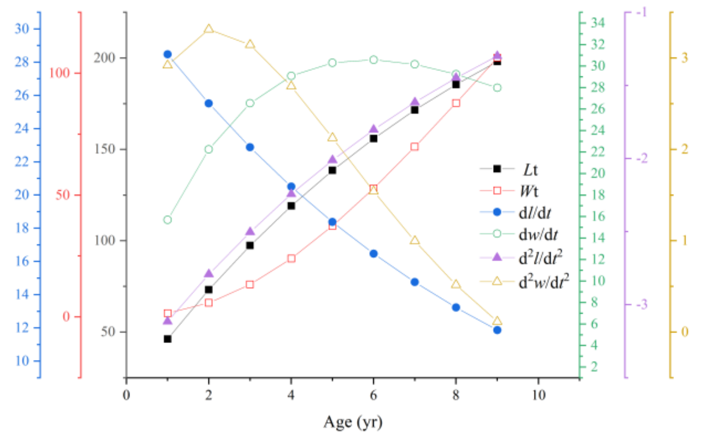

Figure 11. Von Bertalanffy growth/growth rate/growth acceleration of the standard length and weight of the female population in the Hotan River.

3.8. Correlation between Otolith Morphology and Growth in Fish

The association between morphological parameters of otoliths and body weight/standard length was best matched by the logarithmic function according to the principle of minimum AIC value (Tables 3–5). The regression equation was created, and correlation analysis was carried out. R^2 ranged from 0.48 to 0.62, the correlation was not strong, and the fitting effect was not significantly different ($p > 0.05$), but the correlation between standard length and the morphological index of otolith was slightly higher than that between body weight.

Table 3. Comparison of morphological parameters of otoliths with AIC values of different growth equations for standard length.

Morphological Parameter	Linear	Logarithmic	Power	Exponential
OA	−3050.17470	−3052.38664	−3041.71708	−321.12924
R_{max}	−2080.81676	−3749.73248	−3747.55544	−442.77639
R_{min}	−3100.08822	−3120.88221	−3111.15243	114.34746
OP	−1512.86269	−1533.82343	−1524.22967	1598.85819
OL	−2937.54239	−2952.68046	−2945.12256	105.19167
OW	−3524.07473	−3531.11478	−3529.89282	−422.78094

Note: Otolith perimeter (*OP*), otolith area (*OA*), otolith length (*OL*), otolith width (*OW*), the maximum radius of otolith ($R_{max)}$, and minimum radius of otolith (R_{min}).

Table 4. Comparison of morphological parameters of otoliths with AIC values of different growth equations for body weight.

Morphological Parameter	Linear	Logarithmic	Power	Exponential
OA	−291.59416	−3024.81257	−3013.91078	−684.76113
R_{max}	−3626.86108	−3736.8819	−3735.04495	−442.77639
R_{min}	−2911.45940	−3072.18751	−3066.26107	120.35009
OP	−1376.49575	−1507.31532	−1503.05033	1598.85819
OL	−2776.46259	−2909.16640	−2904.39940	111.19148
OW	−3424.90780	−3513.42209	−3512.37929	−422.78094

Note: Otolith perimeter (*OP*), otolith area (*OA*), otolith length (*OL*), otolith width (*OW*), the maximum radius of otolith ($R_{max)}$, and minimum radius of otolith (R_{min}).

Table 5. Relationship between morphological parameters of otolith and body weight/standard length of *H. yarkandensis*.

Relationship between Morphological Parameters of Otolith and Body Weight	R^2	Relationship between Morphological Parameters of Otolith and Standard Length	R^2
$OA = 0.2388\ln W + 0.1690$	0.5605	$OA = 0.72\ln L - 2.5024$	0.5859
$R_{max} = 0.1233\ln W + 0.5094$	0.4822	$R_{max} = 0.3688\ln L - 0.8572$	0.4921
$R_{min} = 0.2423\ln W + 0.6352$	0.5878	$R_{min} = 0.7381\ln L - 2.1076$	0.6168
$OP = 0.6058\ln W + 1.8893$	0.5077	$OP = 1.8297\ln L - 4.9011$	0.5239
$OL = 0.2444\ln W + 0.6206$	0.5909	$OL = 0.7449\ln L - 2.1479$	0.6197
$OW = 0.1289\ln W + 0.5066$	0.4868	$OW = 0.3858\ln L - 0.9232$	0.5012

4. Discussion

4.1. Correlation between Otolith Morphology and Growth in Fish

The extraction of otolith morphological features not only aids in age identification but also serves as a useful tool for taxonomic identification since the deposition of mineral elements in the water column varies in different habitats during the growth and development of aquatic creatures [21]. Fish otolith morphology changes in response to particular gene-guided mechanisms and is also regulated by elements including water temperature, feeding habits, and the amount of bait [22–24]. The morphology and growth of otoliths are determined by the elements that are deposited on them, and otolith growth is linearly associated with the rate of fish growth as the water environment changes [25]. *H. yarkandensis*, which was formerly widely spread across the Tarim River system, lives in habitats with lower habitat temperatures, higher altitudes, and highly salinized and alkaline-degraded water. Fish growth and otolith growth are both slower in waters with extremely little biological bait, which is consistent with research on *Perca fluviatilis* and *Salvelinus malma* by Souza et al. [25] and Morrison et al. [23]. According to this investigation, *H. yarkandensis* only swims into deep water in winter. The shallow depth of the habitat is the primary cause of the tiny size of otoliths, according to Lombarte et al. [26], who noted that the size of otoliths varies proportionally with the depth of the habitat.

Otolith radius regression can be used to quantify fish development in fish age identification, demonstrating a linear relationship between fish growth and otolith morphological structure [27–29]. The R^2 in statistical analysis can reflect the level of its correlation. In the present study, the R^2 between otolith morphology and standard length/body weight of *H. yarkandensis* was less than 0.7. The correlation between standard length/body weight and otolith morphology of *Perca fluviatilis* and *Salvelinus malma* was studied by Battaglia et al. [30] and Souza et al. [25], and in both studies, R^2 was greater than 0.8. The correlation between standard length/body weight and otolith morphology of *Gadus chalcogrammus* was studied by Duan et al. [31], where the R^2 was only 0.5. This is a similar phenomenon to the lower correlation in the present study. Morrison et al. [23] indicated that the cause of this phenomenon is the migratory behavior of fish. When fish migrate to a better water environment with more nutritious bait, their behavior changes as a result. This is consistent with the biological compensatory growth theory, which states that fish tend to accelerate growth when recovering from full or partial food deprivation [32,33]. Otolith growth anisotropy results from the inability to achieve quick mineral element deposition in the water column, short residency times in migratory areas, and incomplete presentation of the organism's accelerated growth in otolith growth. *H. yarkandensis* displayed grabbing behavior before traveling to spawn in a study by Chen [13], and short-term rapid compensatory growth impacted the association between otolith and fish growth. All of the aforementioned investigations provided evidence that the primary factor influencing the relationship between otolith and fish growth in *H. yarkandensis* was their short-distance migration behavior under habitat fragmentation.

4.2. Age Identification Analysis

In fishery resource surveys and assessments, fish age identification analysis is the classic method used to study fish population structure. There are typically two types. The first is to estimate the age of fish using the frequency distribution of standard length, but this method is only applicable to fish with simple age structures or fast growth rates, and the back calculation result is frequently smaller than the actual measured value. The other is to analyze hard tissues such as otoliths, which has been conducted in many studies, including the current one. The pigmentation of hard tissues such as otoliths is influenced by intrinsic factors such as fish species, genetics, and developmental period as well as by external factors such as the habitat environment. This leads to different variations in whorls [34–36], and these variations affect the accuracy of fish age identification. Therefore, the best material for age determination varies from fish to fish [37].

Many academics have compared different fish age identification methods in their studies. Vertebrae, the main material used for age identification, do not require grinding and are easily accessible [38,39]. Dorsal fin spines, gill cover bones, and scales are easily accessible but easily damaged, causing data loss, and they can be used only with other materials for identification [40]. Otoliths are more accurate and reliable as age materials in slow-growing and older fish [14], such as *Ptychobarbus dipogon* in the Tibet autonomous region [41] and *Leuciscus waleckii* in Dali Lake [42]. In the age identification of *Triplophysa*, otoliths and spinal bones have shown higher accuracy. Chen and Zeng et al. confirmed that lapillus otoliths are the best age identification material for *H. yarkandensis*, so these otoliths were chosen as the identification material in this study [13,43].

Based on the alternating light and dark microstructure of otoliths, the age of fish was judged by combining the annual cycle of formation and the position of the first whorl. Jia et al. [44] found that the daily growth whorl appeared at 7–8 months during the rapid growth period of fish. The number of daily whorls observed in this study ranged from 52 to 176, which was a low value. That is, the number of daily wheels observed in this study was lower than the theoretical value. Huo [17] noted that low water temperatures in spring and winter cause the growth of fish to slow or stagnate, which is followed by the narrowing of the transparent band during the formation of otolith whorls. Due to the limitation of optical microscope resolution, it is difficult to distinguish all of the day whorls. Thus, it is reasonable to observe that the number of day whorls observed in this experiment is likely lower than the theoretical value.

In fish ecology studies, age structure analysis is the basis for assessing fishery population changes and constructing resource models [12,45]. Some studies have identified 10 age groups in the *H. yarkandensis* population (3.00–28.00 cm, 10.796 $\pm$ 0.089 cm) in the upper section of the Tarim River, with most individuals determined to be aged 4+ years. In the present study, seven age groups were identified in the Hotan River population (43.34–177.24 mm, 80.65 $\pm$ 20.86 mm), and most were age 2^+ individuals. The large gap between the two groups indicates that the upper Tarim River population has a more complete population structure but is missing a significant number of younger individuals. The Hotan River population has more stable germplasm resources. This was closely related to the fact that the Hotan River flows through the Taklamakan Desert, which has little human activity and a more stable water ecosystem. In addition, the feeding needs of *H. yarkandensis* were guaranteed to some extent by bait organisms [42].

4.3. Growth Characteristics Study

The growth and development of fish are greatly influenced by factors such as species and habitat environment. Different fish populations have different growth patterns [12,18]. Compared with the growth characteristics of *H. yarkandensis* measured in the Tarim River and Yarkand River at the same time [46], the inflection point ages of the Tarim River (L_∞ = 108.7105, W_∞ = 24.4995, $t_0 = -1.7239$, t_i = 1.8295) and Yarkand River populations (L_∞ = 166.5742, W_∞ = 56.6625, $t_0 = -1.319$, t_i = 3.9548) had a significantly younger age of inflection than that of the Hotan River population (L_∞ = 302.772, W_∞ = 310.8450, $t_0 = -0.4608$, t_i = 9.0710). The age of sexual maturity may be earlier with signs of early maturity, which may be closely related to the trend of population miniaturization exacerbated by water degradation in the Tarim River. The young age of the Tarim River population is closely related to the increase in the salinity, sand content, and water volume of the Tarim River in recent years, as well as the influence of human activities [10,47]. The young age of the Yarkand River population has been influenced by the excessive construction of water hubs along the basin, the canalization of rivers, the continuous increase in the area of cultivated land in the basin, and the introduction of exotic species. Three sites (spawning grounds, etc.) of *H. yarkandensis* have been destroyed. Growth has been restricted, and the growth inflection point has changed.

Comparing the t_0 values under ideal conditions, the populations of the Tarim River and Yarkand River are smaller than the population of the Hotan River. This result indicates that their development is more advanced. It also reflects, to varying degrees, the problems of environmental degradation of water bodies and safety hazards in critical habitats.

In this study, the mean Fulton condition index of the *H. yarkandensis* population in the Hotan River was not significantly different from that of the Tarim, Kezi, and Akesu River populations ($p > 0.05$). The Fulton condition index showed that there were slightly more males than females, which was consistent with the results of the study by Chen. He showed that the *H. yarkandensis* in the upper section of the Tarim River had a large variation in mean age growth, significant interannual variation, a serious lack of young individuals, significant differences between males and females ($p < 0.05$), and a clear trend toward miniaturization [13,19,42,46]. This phenomenon was in accordance with the general pattern of fish growth. *H. yarkandensis* has been affected by individual miniaturization, and the male base is larger in the lower age groups, causing a phenomenon in which males have higher fecundity than females.

Among *Triplophysa*, *T. siluroides* in the Qinghai Basin, *T. tenuis* in the Kaidu River, and *T. bombifrons* in the Tarim River all exhibited anisotropic growth, which is reflected by a thin body, unstable growth, and an obvious miniaturization trend. However, the *H. yarkandensis* in this study had a uniform growth rate. This was closely related to the fact that the Hotan River flows through the Taklamakan Desert, which has little human activity and a more stable water ecosystem. In addition, the feeding needs of *H. yarkandensis* were guaranteed to some extent by bait organisms [48].

5. Conclusions

In degraded environments, such as alpine climatic conditions and salinized water features, the endangerment of indigenous fishes has intensified. 2^+ individuals accounted for more. The comparative study found that the growth parameters of the Hotan River population (L_∞ = 302.772, W_∞ = 310.8450, t_0 = -0.4608) were higher than those of the other groups. This suggests that the germplasm resources of the Hotan River population have been relatively stable. This is due to the fact that the Hotan River is less affected by human activities and the feeding needs of the population are secured.

Author Contributions: X.-Y.W. drafted the manuscript. C.-X.W. and F.L. designed the study and performed the statistical analysis. S.-A.C. and Y.S. conceived of the study and participated in its design and coordination. S.-A.C. gave final approval of the version to be published. All authors have read and agreed to the published version of the manuscript.

Funding: This study was funded by the Natural Science Foundation of China (no. 31360635), the Key Tackling Project of science and Technology Bureau of Xinjiang Production and Construction Corps (no. 2022DB019), the Special Agriculture and Rural Finance Project (Investigation on Fishery Resources and Environment in Key Waters of Northwest China), etc.

Institutional Review Board Statement: The animal study protocol was approved by the Ethics Committee of College of Animal Science and Technology, Tarim University (protocol code TDD-KYXF20180225 and date of approval 25 February 2018).

Informed Consent Statement: Not applicable for studies not involving humans.

Data Availability Statement: The link to the data is not yet publicly available because the project has not been finalized.

Acknowledgments: We would like to thank our colleagues of the Fishery Department. Thanks to Yingcheng Studio for providing the language touch-ups for this article.

Conflicts of Interest: The authors declare that they have no competing interest.

References

1. Sun, B.G.; Mao, W.Y.; Feng, Y.R.; Chang, T.; Zhang, L.P.; Zao, L. Study on the Change of Air Temperature, Precipitation and Runoff Volume in the Yarkant River Basin. *Arid Zone Res.* **2006**, *23*, 203–209.
2. Nazakaiti, T.; Hudan, T.; Jiao, P.; Milishati, M.; Chen, J. Study on the evolution characteristics of main hydrometeorological factors and runoff in Hetian river basin in recent 60 years. *J. China Hydrol.* **2022**, *42*, 85–89.
3. Zhen, Y.Q. Study on Water Resources Protection Planning of Hotan River Basin. Master's Thesis, Xi'an University of Technology, Xi'an, China, 2005.
4. Song, B.Y. A study on the changes of Khotan River since the Wei and Jin Dynasties. Master's Thesis, Northwest Minzu University, Lanzhou, China, 2018.
5. Záhorská, E.; Kováč, V.; Falka, I.; Beyer, K.; Katina, S.; Copp, G.H.; Gozlan, R.E. Morphological variability of the Asiatic cyprinid, topmouth gudgeon *Pseudorasbora parva*, in its introduced European range. *J. Fish Biol.* **2009**, *74*, 167–185. [CrossRef] [PubMed]
6. Gorgonio, R.C.; Faustino, C.R.; Alejandro, V.R.; Sergio, S.G.; Jorge De La, R.V. Morphometric variation of wild trout populations from northwestern Mexico (Pisces: Salmonidae). *Rev. Fish Biol. Fish.* **2003**, *13*, 91–110.
7. Xie, C.G.; Ma, Y.W.; Guo, Y. Analysis of Biogeography of Fishes in Tarim Basin. *Chin. J. Fish.* **2015**, *28*, 40–46.
8. Zhao, W.H.; Yi, S.K.; Su, J.X.; Zhou, Q.; Shen, J.Z.; Li, D.P.; Zhao, X.Y. Genetic diversity of *Triplophysa Yarkandensis* populations in Tarim river basin in Xinjiang. *Acta Hydrobiol. Sin.* **2022**, *46*, 364–374.
9. Zhao, W.H.; Yi, S.K.; Zhou, Q.; Shen, J.Z.; Li, D.P.; Zhao, X.Y. Population Genetic Study of *Triplophysa yarkandensis* in Tarim River Basin in Xinjiang. *Fish. Sci.* **2023**, *42*, 664–673.
10. Zhao, J.F.; Qiu, L.H.; Zhou, Q.; Zhou, X.Y.; Shen, J.Z. Age structure and growth characteristics of *Triplophysa yarkandensis* in the Qarqan River, Xinjiang. *J. Huazhong Agric. Univ.* **2022**, *46*, 1–9.
11. Wang, X.Y.; Chen, S.A.; Wang, C.X.; Zi, F.Z.; Chang, D.S.; Xu, H.; Li, D.P. Otolith Morphology and Population Discrimination of *Triplophysa yarkandensis*. *Prog. Fish. Sci.* **2023**, *44*, 201–211.

12. Yin, M.C. *Fish Ecology*; China Agriculture Press: Beijing, China, 1995.
13. Chen, S.A. Study on Population Ecology of *Triplophysa yarkandensis* (Day) in Tarim River. Master's Thesis, Huazhong Agricultural University, Wuhan, China, 2012.
14. Steven, E.C.; Simon, R.T. Otoliths, increments, and elements: Keys to a comprehensive understanding of fish populations? *Can. J. Fish. Aquat. Sci.* **2001**, *58*, 30–38.
15. Gaemers, P.A.M. Taxonomic position of Cichlidae (Pisces, Perciformes) as demonstrated by the morphology of their otoliths. *Neth. J. Zool.* **1983**, *34*, 566–595.
16. Haas, R.E.; Recksiek, C.W. Age verification of winter flounder in Narragansett Bay. *Trans. Am. Fish. Soc.* **1995**, *124*, 103–111.
17. Huo, B. Study on the Biology and Population Dynamics of *Oxygymnocypris stewartii*. Ph.D. Thesis, Huazhong Agricultural University, Wuhan, China, 2014.
18. Pauly, D. The relationship between gill surface area and growth performance in fish: A generalization of von Bertalanffy's theory of growth. *Meeresforsch* **1981**, *28*, 251–282.
19. Ren, B.; Ma, Y.W.; Tu, E.X.; Guo, Y.; Zhang, R.M.; A, B.D.; Ai, Z.Z.; Liu, Y. The study on the biology of *Triplophysa* (Hedinichthgs) *yarkandensis* (Day) in Akesu River. *Chin. J. Fish.* **2004**, *17*, 46–52.
20. Ma, B.S. Study on the biology and population dynamics of *Schizothorax O'connori*. Ph.D. Thesis, Huazhong Agricultural University, Wuhan, China, 2011.
21. Sergio, B. Fish age classification based on length, weight, sex and otolith morphological features. *Fish. Res.* **2007**, *84*, 270–274.
22. Ding, L.; Tao, J.; Ding, C. Hydrogeomorphic factors drive differences in otolith morphology in fish from the Nu-Salween River. *Ecol. Freshw. Fish* **2019**, *28*, 132–140.
23. Morrison, C.M.; Kunegel, L.M.; Gallagher, C.P. Decoupling of otolith and somatic growth during anadromous migration in a northern salmonid. *Can. J. Fish. Aquat. Sci.* **2019**, *76*, 1940–1953. [CrossRef]
24. Miloevi, D.; Bigovi, M.; Mrdak, D. Otolith morphology and microchemistry fingerprints of European eel, Anguilla anguilla (Linnaeus, 1758) stocks from the Adriatic Basin in Croatia and Montenegro. *Sci. Total Environ.* **2021**, *786*, 147478.
25. Souza, A.T.; Soukalova, K.; Ded, V. Ontogenetic and interpopulation differences in otolith shape of the European perch (*Perca fluviatilis*). *Fish. Res.* **2020**, *230*, 105673. [CrossRef]
26. Lombarte, A.; Cruz, A. Otolith size trends in marine fish communities from different depth strata. *J. Fish Biol.* **2007**, *71*, 53–76. [CrossRef]
27. Zhang, T.; Wang, H.H.; Bi, X.J. Sagittal otolith growth and development at different development stages in larval and juvenile *Coilia mystus* in the Yangtze estuary. *J. Fish. Sci. China* **2017**, *24*, 1315–1322. [CrossRef]
28. Ma, Q.Y.; Xue, Y.; Xu, B.D. Relationships between otolith size and fish size for twelve prey fish species from Jiaozhou bay. *Acta Hydrobiol. Sin.* **2013**, *37*, 481–487.
29. Peng, L.; Jiang, Y.E.; Xu, S.N. Otolith morphology of *Nemipterus virgatus* and its relation to body length and mass in continental shelf of northern South China Sea. *South China Fish. Sci.* **2018**, *14*, 27–33.
30. Battaglia, P.; Malara, D.; Romeo, T. Relationships between otolith size and fish size in some mesopelagic and bathypelagic species from the Mediterranean Sea (Strait of Messina, Italy). *Sci. Mar.* **2010**, *74*, 605–612. [CrossRef]
31. Duan, M.; Wei, L.; Zhu, G.P. Morphometric features of sagittal otolith for Alaska pollock *Gadus chalcogrammus* in the western Bering Sea. *J. Dalian Ocean Univ.* **2018**, *33*, 492–498.
32. Fey, D.P. The effect of temperature and somatic growth on otolith growth the discrepancy between two clupeid species from a similar environment. *J. Fish Biol.* **2006**, *69*, 794–806. [CrossRef]
33. Mangel, M.; Munch, S.A. Life-History Perspective on Short-and Long-Term Consequences of Compensatory Growth. *Am. Nat.* **2005**, *166*, E155–E176. [CrossRef]
34. Mitsui, S.; Strussmann, C.A.; Yokota, M.; Yamamoto, Y. Comparative otolith morphology and species identification of clupeids from Japan. *Ichthyol. Res.* **2020**, *67*, 502–513. [CrossRef]
35. Campana, S.E. How Reliable are Growth Back-Calculations Based on Otoliths? *J. Can. Des Sci. Halieut. Et Aquat.* **1990**, *47*, 2219–2227.
36. Zhang, X.J.; Chen, J.H. Survey on study of the fish age determination. *Mar. Fish.* **2009**, *31*, 92–99.
37. Polat, N.; Bostanci, D.; Yilmaz, S. Comparable Age Determination in Different Bony Structures of *Pleuronectes flesus luscus* Pallas, 1811 Inhabiting the Black Sea. *Turk. J. Zool.* **2001**, *25*, 441–446.
38. Liu, S.P. A study on the biology of *Pseudobagrus fulvidraco* in Poyang Lake. *Chin. J. Zool.* **1997**, *32*, 10–16.
39. Duan, Z.H.; Sun, J.Y. Study on the age and growth of *Pelteobagrus vachelli* (Richardson). *Acta Hydrobiol. Sin.* **1999**, *23*, 617–623.
40. Zhu, X.F.; Chen, Y.F. Preliminary study on the age and growth characteristics of *Schizothorax macropogon*. *Chin. J. Zool.* **2009**, *44*, 76–82.
41. Liu, Y.C.; Liu, S.Y.; Liu, H.P. Values of eight structures as age determination of *Ptychobarbus dipogon*, Tibet autonomous region. *Acta Hydrobiol. Sin.* **2019**, *43*, 579–588.
42. Cai, Z.L.; Duan, Y.J.; Xu, J.C.; He, Y.; Geng, J.Z.; Liu, X.; Han, M.X.; Liu, Y.H. Comparison of five structure meterials in age determination of Amur ide *Leuciscus waleckii* in Dali Lake. *J. Dalian Ocean Univ.* **2020**, *35*, 121–125.
43. Zeng, L.; Tang, W.Q. Discussion on age determination methods for two esquamate *Triplophysa* fishes. *Chin. J. Zool.* **2010**, *45*, 94–103.
44. Jia, Y.; Chen, Y. Otolith microstructure of *Oxygymnocypris stewartii* (Cypriniformes, Cyprinidae, Schizothoracinae) in the Lhasa River in Tibet, China. *Environ. Biol. Fishes* **2009**, *86*, 45–52. [CrossRef]
45. Zeng, L.; Tang, W.Q. Age, body, growth and reproductive characteristics of *Triplophysa yarkandensis*. *Chin. J. Zool.* **2010**, *45*, 29–38.

46. Wang, X.Y. Age, Growth, Reproduction and Population Discrimination of *Triplophysa yarkandensis*. Master's Thesis, Tarim University, Alar, China, 2022.
47. Chen, S.A.; Yao, N.; Ren, D.Q.; Xie, C.X.; Fan, Z.M. Study on the population structure of *Triplophysa* (Hedinichthys) *yarkandensis* (Day) in the upper reaches of Tarim river. *J. Northeast Agric. Univ.* **2014**, *45*, 90–97.
48. Chen, S.A. Early Development and Physiological Mechanism of Salinity-Alkalinity Adaption of *Triplophysa yarkandensis* (Day). Ph.D. Thesis, Huazhong Agricultural University, Wuhan, China, 2019.